Shallow Crustal Structure Beneath Taal Volcano, Philippines, Revealed by the 1993 Seismic Explosion Survey

By Kin'ya NISHIGAMI, Takuo SHIBUTANI, Takahiro OHKURA, Masaya HIRATA, Haruo HORIKAWA, Kouichi SHIMIZU, Shigemitsu MATSUO, Setsuro NAKAO, Masataka ANDO, Bartolome C. BAUTISTA, Ma. Leonila P. BAUTISTA, Edito S. BARCELONA, Ramses VALERIO, Angelito G. LANUZA, Arnold V. CHU, Jason Jude VILLEGAS, Ariel R. RASDAS, Enrico A. MANGAO, Elmer GABINETE, Baby Jane T. PUNONGBAYAN, Ishmael C. NARAG, Felix MARTE and Raymundo S. PUNONGBAYAN

(Manuscript received on March 16, 1994, revised on September 27, 1994)

Abstract

We carried out an seismic explosion survey at Taal volcano in March, 1993. The explosions were done at the west of the volcanic island and digital event recorders were deployed along a fan-shooting survey line at the east of the volcanic island and also along a short straight survey line across the island. Small-aperture arrays were also operated at two sites west of the volcanic island. We found that P waves that traveled just beneath the main crater strongly attenuated and showed later arrivals. This result suggests the existence of a low-velocity and low-Q region around the main crater at a depth of about 1.5 km, although the location and extent cannot be determined exactly. P wave velocity of this abnormal region may be eatimated to be lower than that of the surroundings by much greater than about 25%, if we assume the region is restricted just beneath the main crater. We applied the NMO correction to the later part of seismograms and found a reflector around the east of the main crater at a depth of about 6 km, which may suggest the top surface of the magma reservoir.

1. Introduction

It is important to investigate the heterogeneous crustal structure below active volcanoes, especially the location and extent of magma bodies, in order to understand the basic structure and the state of activity of the volcanoes and also to predict the forthcoming eruption.

Seismic data obtained by dense networks concentrated around active volcanoes have revealed the heterogeneous structure below them. The location of magma reservoirs or conduits below active volcanoes is estimated by detailed analyses of the hypocentral distribution of volcanic earthquakes, the anomaly of travel times and amplitude of seismic waves, crustal movements accompanying the eruption, and other geophysical observations (e.g., Ishihara, 1988). 3-D seismic tomography using local and teleseismic earthquakes has revealed low velocity areas existing just beneath active volcanoes (e.g., Achauer et al., 1986; Zhao et al., 1992; Mikumo et

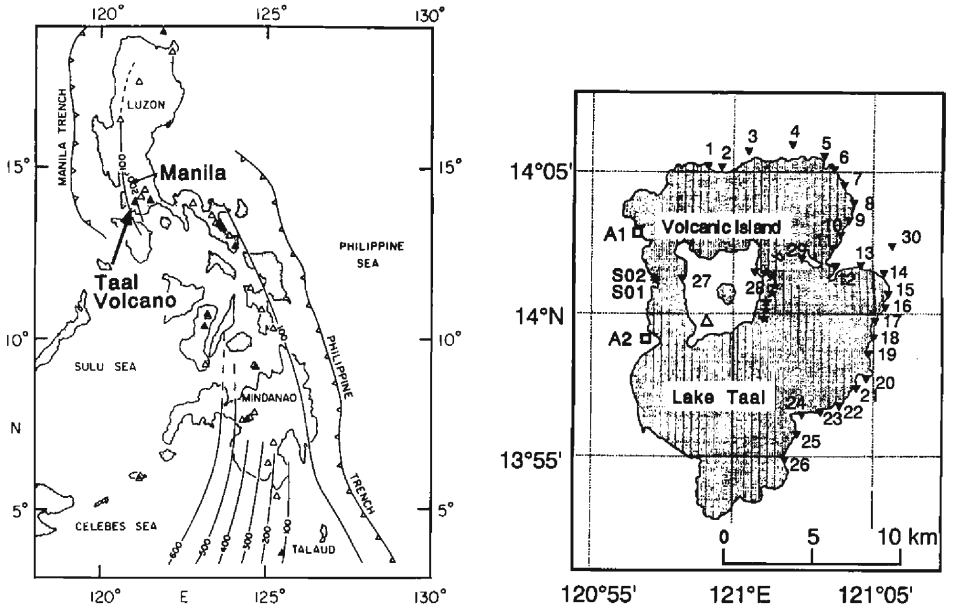

(a) (b)

Fig. 1. (a) Map showing the tectonic setting of the Philippine Islands (modified from Cardwell et al., 1980). Depth contours in km represent the tops of the inclined seismic zones. Historically active volcanoes are shown as solid triangles, and volcanoes of inferred Quaternary age are shown as open triangles. Taal Volcano is indicated by the solid one with an arrow. (b) Map showing the location of shot points (S01 and S02), fan-shooting stations (No. 1–26), short-line stations (No. 27–30), and array sites (A1 and A2) installed around Taal Volcano. Stars indicate the surface projection of the location of possible reflectors estimated by the NMO correction analysis. The open triangle on the volcanic island shows the location of Mt. Tabaro, a recent eruption site.

al., 1993).

On the other hand, seismic prospecting using artificial explosions has also been done extensively in order to elucidate the shallow heterogeneous structure in the volcanic areas. Anomalous region in velocity and attenuation is detected by fan-shooting observation (e.g., Ono et al., 1978 ; Moriya and Okada, 1980 ; Ueki et al., 1990). Fine 3-D structure of velocity and attenuation is revealed by seismic tomography (e.g., Ankeny et al., 1986 ; Achauer and Evans, 1988 ; Evans and Zucca, 1988). Magma reservoirs at deeper part can be detcted by the reflection method (e.g., Brown et al., 1980 ; Hill et al., 1985).

The present paper describes the seismic explosion survey at Taal Volcano in 1993, where fan-shooting, refraction, and reflection methods were used with a view to detecting molten magma body which may exist below the volcano.

Taal Volcano is one of the most active volcanoes in Philippines, located about 60 km south of Manila in Luzon Island. **Figure 1(a)** shows the tectonic setting of the Philippine Islands. Taal Volcano appears to be associated with the Manila Trench subduction (Cardwell et al., 1980). The volcano is composed of a volcanic island with extent of about 5×5 km^2 and

summit elevation of 311 m, and the caldera lake named Lake Taal surrounding the island (**Fig. 1(b)**). There exists a main crater with a diameter of about 2 km at the center of the volcanic island and a crater lake inside it. The eruptions of Taal Volcano have been recorded more than 30 times since 1572, and recently many people were killed by its great magmatophreatic eruption in 1911 and 1965. The process of the 1965 eruption is reported in detail by Nakamura (1966). The eruption in 1965 and some eruptions after that occurred at Mt. Tabaro, southwest of the main crater as indicated in **Fig. 1(b)**. No eruption has occurred since the last phreatic eruption in 1977, although volcanic earthquakes or crustal movement is observed in 1987–1989, and 1991–1992 and the inhabitants were sometimes evacuated from the volcanic island. During the latest activity in February, 1992, a fissure with about 1 km length in east–west direction appeared at the northern foot of the main crater and steaming has been observed along it.

A seismic explosion survey was performed in the Taal Volcano area during 27 February–8 March, 1993 by the Joint Research Group of Kyoto University and Philippine Institute of Volcanology and Seismology (PHIVOLCS). The explosions were carried out at two sites west of the volcanic island (**Fig. 1(b)**), using 200 kg of explosives inside the boreholes. Digital event recorders were installed along a fan–shooting survey line at the east of the volcanic island and also along a short straight survey line across the island. Small–aperture arrays were also operated at two sites west of the volcanic island.

Purposes of the explosion survey at Taal Volcano were as follows : (1) To obtain average P velocity structure in the shallow crust (about 0–2 km in depth) by the refraction method, (2) To estimate velocity and attenuation anomalies at shallow depths (about 1 km) of Taal Volcano by detecting spatial variation in travel times and amplitudes of direct P waves, (3) To estimate the location and property of reflecting materials at deeper part (deeper than about 2 km) below the volcano by analyzing coda waves, and (4) To estimate the location of strong scatterers or reflectors below Taal Volcano by analyzing coda waves observed at array stations. These results will provide information about heterogeneous structure, which may include magma reservoirs, below Taal Volcano. The result of (1) will also be useful in determining hypocenters of shallow volcanic earthquakes.

Since the activity of volcanic earthquakes was very low during this survey, seismic prospecting using those earthquakes was not added to the survey plan. This survey was the first trial in the Philippines to explore shallow crustal structure by artificial explosions. So, in this paper, some technical notes about the explosion will also be given in detail.

2. Observation

2.1 Shot point

(1) Explosion

Shot points were built at two places on the west shore of Lake Taal, about 500 m distant from the nearest village (**Fig. 1(b)**). Locations of the shot points are shown in **Table 1**. The distance between the two points, about 200 m, is short enough compared with the epicentral distance to the observation stations and can be ignored in analyzing travel times or waveforms

Table 1. Locations and shot times in the local time for the two shots

shot	*Latitude*	*Longitude*	*Time*
1	14° 01′ 11.2″ N	120° 57′ 15.1″ E	23h 00m 00.090s, Mar.2, 1993
2	14° 01′ 17.3″	120° 57′ 12.0″	23h 00m 02.316s, Mar.5

in the present study. Both explosions were observed at two stations as will be described later, and the similarity of their waveforms and P arrival times were practically recognized.

Three boreholes were drilled by GEOTECHNICS PHILIPPINES, INC. The diameter was 6 inches (15 cm) and the maximum depth was scheduled to be 50 m. The drilling was not easy, however, because a porous sand layer was encountered at a depth of about 18 m. Finally, the borehole of 50 m depth was adopted for the first explosion and another one of 29 m depth was for the second shot. A metal casing of 12 m length was put inside them to prevent the collapse of soft surface soil and the casing was fixed to the ground by concrete with iron stakes.

The drilled hole was filled with water rich in bentonite even after washing by injecting the lake water. Therefore, the explosives did not sink under their own weight. In the case of 50 m borehole, the deepest point of a cartridge filled with explosives was only 20–30 m. As a result, water pressure of about 10 m was applied to the explosives for both shots, with the expection of increasing the efficiency of seismic wave radiation.

The explosion was operated by GOLDFIELD CONSTRUCTION DEVELOPMENT CORP. We used explosives called "EMULITE 150" produced by NOBEL PHILIPPINES, INC., which was supposed to be safe and applicable for underwater blasting. The "EMULITE" has the following properties: density, 1.2 gm/cm^3; weight strength, 107% against ANFO; detonation velocity, 5.5 km/sec; weight, 1 kg/piece; resistance to water, 1 month under normal conditions and 1 week under high hydrostatic pressure. ANFO is a kind of explosive used for quarry blasting because of its low detonation velocity. The total weight of explosives was 200 kg for each shot. They were devided into about 12 cylindrical cartridges, each of which was 1 m in height.

The explosives called dynamite are generally used for seismic explosion experiments in Japan. Dynamite has a density of about 1.5, weight strength of 120% against ANFO, and detonation velocity of 5.0–6.0 km/sec. The "EMULITE" used in this survey has almost the same properties as dynamite, except for a little smaller density.

(2) Measurement of shot time

The shot time is one of the most important items of data in seismic explosion experiments. In this survey, the shot time was measured by observing three different signals accompanying the explosions, as shown in **Fig. 2**. The first signal, seismic waves, were observed by a velocity transducer with a natural frequency of 4.2 Hz installed on the ground surface just beside the borehole, and were recorded with high and low amplifications. The second signal was the

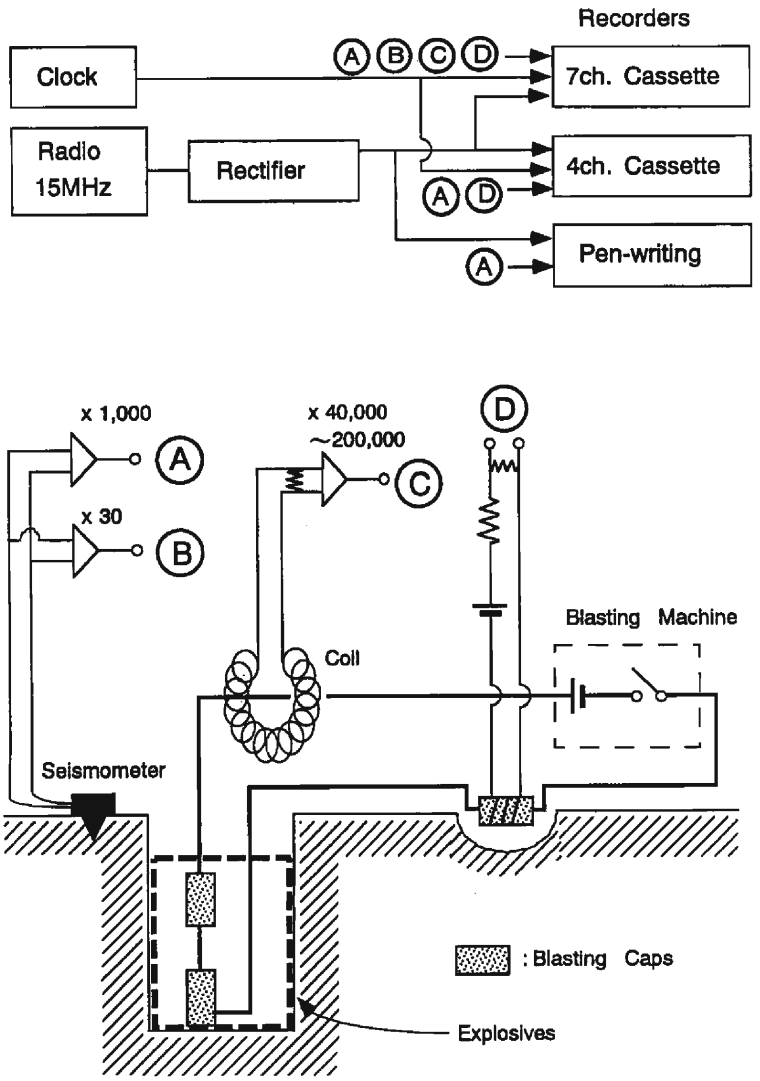

Fig. 2. Schematic diagram showing the observation of shot time. Ground motion detected just beside the borehole, induced voltage to a coil, and breakage of the blasting cap on the ground are recorded by three kinds of recorders with BSF time code.

breakage of blasting caps. Two blasting caps were connected in series at the top and bottom of the explosives. Another blasting cap was connected in series with them and buried in about 30 cm depth outside a borehole. A thin leading wire was wound around the third blasting cap, and some voltage was applied to the wire with feeble electric current. The three blasting caps are expected to be broken simultaneously and its time was recorded as the change of voltage applied to the leading wire. The third signal was the induced voltage to a coil surrounding the electric wire that connected three blasting caps. These three kinds of signals were recorded

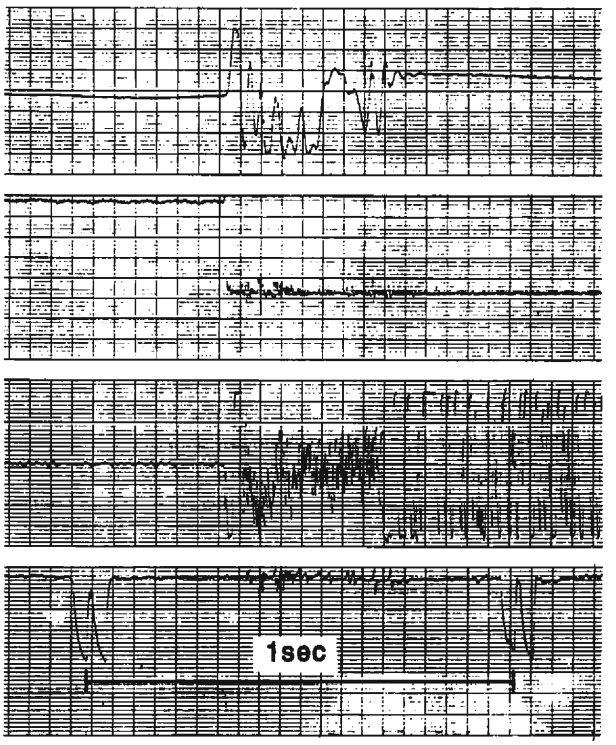

Fig. 3. Observed records of shot time measurement for the second explosion. Top to bottom: induced voltage to a coil, break of a blasting cap, seismic signals, and rectified BSF time code.

with rectified BSF time code and a clock signal. We used two analogue cassette-tape recorders, a 7-channel FM recorder (HR-30G, TEAC) and a 4-channel FM recorder (R-70A, TEAC), to prevent failure in operation. BSF time code, which is broadcasted from Taiwan at 15 MHz, was received by a radio and it was used for the common time signal at the shot point and all the observation stations. High-gain seismic waves and BSF code were also monitored by a paper-writing recorder. All the recording systems were operated by dry batteries and a car battery (12 V).

Observed records for the second shot are represented in **Fig. 3**. The three signals stated above seem to have almost the same onset time. Since the induced voltage shows somewhat gradual increase, we read the time of the brake of a blasting cap by comparing it with the seismic signal. The shot times thus obtained are shown in **Table 1**. The accuracy is estimated to be about 2 msec for the second shot, and 5-10 msec for the first one because of a little noisy BSF signal.

After the explosion, the metal casing showed an upward motion of about 0.5 or 2 m for the two shots. A hole with a diameter of about 3 m and a depth of about 1 m appeared around the borehole of the second shot.

2.2 Fan-shooting and short-line stations

Fan-shooting stations (No. 1–26) were installed at about 1 km intervals along the east shore of Lake Taal, and short-line stations (No. 27–30) were at 4 points including the volcanic island (**Fig. 1(b)**). Since we used only 16 event-recorders in this survey, stations 1–16 and 17–30 were operated for the first and the second explosion, respectively. Both of the two explosions were observed at stations 1 and 13 to calibrate the amplitude of the records between the two shots.

Vertical components of velocity-type transducers with a natural frequency of 2 Hz (L-22 D, Mark Products) were used at every station. Waveforms were digitized at 400 Hz with 12 bits and recorded in floppy disks by using digital recorders (EDR-1000 and EDR-1300, Kinkei System). All of the instruments were operated by car batteries and the recording was controlled by an internal timer at the scheduled shot time and some spare shot times. The responses of all the seismometers were calibrated by using a shaking table and the sensitivity of recorders were also calibrated by inputting the test signals. The station locations were measured from a topographic map of scale 1/50,000 by referring to those positioned by a portable GPS receiver.

2.3 Array stations

We made small-aperture array observations with a view to detecting reflected or scattered waves from heterogeneity which may exist in the vicinity of Taal Volcano. Array stations were deployed at two sites on the west shore of Lake Taal as shown in **Fig. 1(b)**. A1 array was operated for the first shot and A2 for the second one. Seismometers were settled on a rock site along the lake shore at A1 array, but buried at a depth of about 30 cm in the rice field at A2 array. Each array consisted of five stations with aperture of about 100–200 m, and had one three-component station and four vertical-component stations. Seismometers were the same as used for the fan-shooting stations and also calibrated in the same way. The wave signals were digitized at 1 kHz with 14 bits and recorded by using a digital recorder (DRF1, TEAC).

3. Results and discussion

3.1 Average P-wave velocity structure

The blasting was carried out at 11 p.m. on 2 and 5 March, 1993 and waveform records were successfully obtained at all the stations.

Seismograms were somewhat noisy at several stations where transducers were buried underground and we applied the 1–16 Hz band-pass filter to all the records in the present analysis.

Figure 4 shows the seismograms obtained at all the fan-shooting and short-line stations. One of the seismograms recorded at A1 array is also plotted. Although the data are not sufficient near the shot point, we estimated the average P wave velocity structure at the shallow crust by assuming a three-layer model. Two solid lines were obtained by the least squares method. Travel times within the surface layer may have large uncertainty from those tenta-

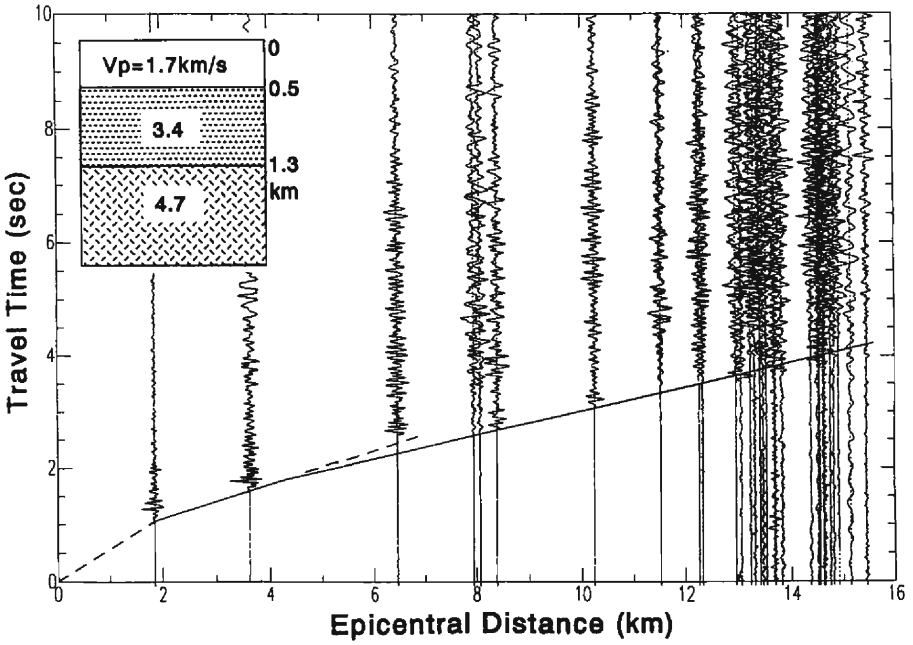

Fig. 4. Seismograms recorded at fan-shooting and short-line stations and one of the A1 array stations, plotted against epicentral distances. The inset shows the estimated P wave velocity structure.

tively plotted by the broken line. The structure thus obtained is as follows: the surface layer with velocity of 1.7 km/s and thickness of about 0.5 km, the second layer with 3.4 km/s and thickness of 0.8 km, and the third layer with 4.7 km/s. Since the largest epicentral distance is 15 km in our survey, the maximum depth that we can prospect is supposed to be about 2 km or so. The velocity in the surface layer is estimated as 1.7 km/s or less, near to that of acoustic waves in water. The shallow part of the volcano may contain a water-filled structure and this supposition may explain the magmatophreatic eruptions that often occur at Taal Volcano. Nakamura (1966) also considered the existence of lake water below the volcanic island as being one of the imporatnt factors of magmatophreatic eruptions.

S phases seem not to be recognizable in **Fig. 4**, probably because of the vertical component of seismograms as well as the explosive source.

3. 2 Abnormal region of P-wave amplitude and velocity

Travel time residuals from the average structure are represented in **Figs. 5** and **6**. The horizontal axis in **Fig. 5** indicates the azimuth of stations measured from the shot point. The rim of the main crater ranges about between 80° and 110°, and the stations 13, 16–19 and 28 that correspond to this range and show later P arrivals are denoted by the squares in **Fig. 5**. These stations show delays in P arrival times by up to about 0.25 sec. On the other hand, the stations 21–25, greater than 120° in azimuth, show relatively faster P arrivals and the boundary at about 120° is very remarkable.

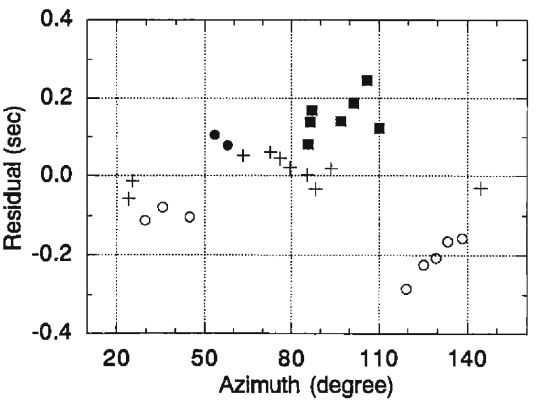

Fig. 5. P wave travel time residuals from the average structure model shown in **Fig. 4**, plotted against the azimuth of stations from the shot point. Open and solid symbols represent faster and later arrivals than the average, respectively, and crosses show residuals less than 0.06 sec. Solid squares indicate the stations 13, 16–19 and 28, where seismic waves travel just beneath the main crater.

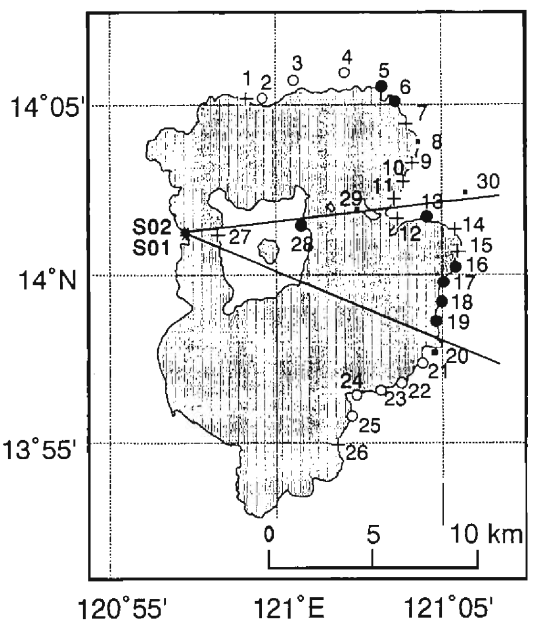

Fig. 6. P wave travel time residuals plotted for fan–shooting and short–line stations. Symbols are the same as in **Fig. 5**, except stations 13, 16–19 and 28 where solid circles are used. P arrivals could not be read at stations shown by the dots. The region between the two solid lines indicates a possible extent of low velocity area.

Although the initial motion of P waves have small onset at every station, we can recognize spatial variation in their amplitudes as will be shown in **Fig. 7**. The amplitude of initial P waves is relatively large at stations 22–26 (azimuth 125°–145°), very small and almost invisible

at stations 12–19 (85°–110°), and intermediate at stations 1–11 (25°–80°). The epicentral distances are almost the same for stations 12–19 and 22–26, and this amplitude distribution is considered to be caused by the lateral variation of attenuation property in the crust. These results suggest the existence of a low-velocity and low-Q region around the main crater. Its depth is estimated to be about 1.5 km because initial P waves travel along the top of the third layer for these stations.

We cannot estimate the exact location and extent of the low velocity region inside the fan-shaped area shown in **Fig. 6** only by the present survey. If we suppose the abnormal region exists just below the main crater, the horizontal extent can be evaluated as about 2 km. The average delay of P arrivals is about 0.15 sec as shown in **Fig. 5**, and this region exists in the third layer of 4.7 km/s. From these, P wave velocity of this region is estimated to be about 25% lower than the average structure. In this evaluation we should notice that the average structure of 4.7 km/s was obtained by including P arrivals delayed by the low-velocity region as shown in **Fig.5**. Therefore, the velocity contrast between the low-velocity and its surrounding regions is estimated to be much greater than 25%.

3.3 Reflection phase

Next, we analyze the later part of seismograms, the coda part, with a view to detecting reflection phases which will give us information about deeper structures below the volcano. In the present study, we used the normal moveout (NMO) correction method in three-layered structure model obtained above. For the stations where refracted waves from the third layer appear as first arrivals, phases in the early part of seismogrms may be interpreted as reflected waves from some reflectors existing inside one of the three layers. The travel times of reflected waves change little if they are from reflectors inside a thin and low-velocity surface or the second layer such as in the present case. Therefore, it is difficult to find reflectors in the surface or the second layer, and thus we try to detect reflectors only in the third layer in this study.

Waveforms after NMO correction are shown in **Fig. 7** in azimuthal sequence. The effect of anelastic attenuation has not been corrected because some later phases could be seen with relatively large amplitude. Two kinds of later phases are found at depths about from 6 to 8 km as indicated in the inset in the figure; the shallower one (*A*) at a depth of about 6 km is seen mainly at stations 13–19, and the deeper one (*B*) at a depth of about 7–8 km is seen at almost all the stations. We examined the apparent velocity of these phases. Phase *A* has a higher apparent velocity than the first P arrivals at stations 13–19, and therefore, this phase can be interpreted as reflected waves from a depth of about 6 km. On the other hand, the apparent velocity of phase *B* is lower than that of the initial P arrivals and nearly the same as that of the refracted waves at the second layer. Phase *B* cannot be interpreted as reflected waves from any reflectors inside the third layer. From these results, we can suppose some reflective materials with strong impedance contrast at a depth of about 6 km. The surface projection of possible reflection points, i.e., the mid points between shot points and stations 13–19, are plotted in **Fig. 1(b)**. The estimated reflector lies only around the east of the main crater and may suggest the top surface of a magma reservoir.

We examined several structure models in NMO correction. The results show similar pat-

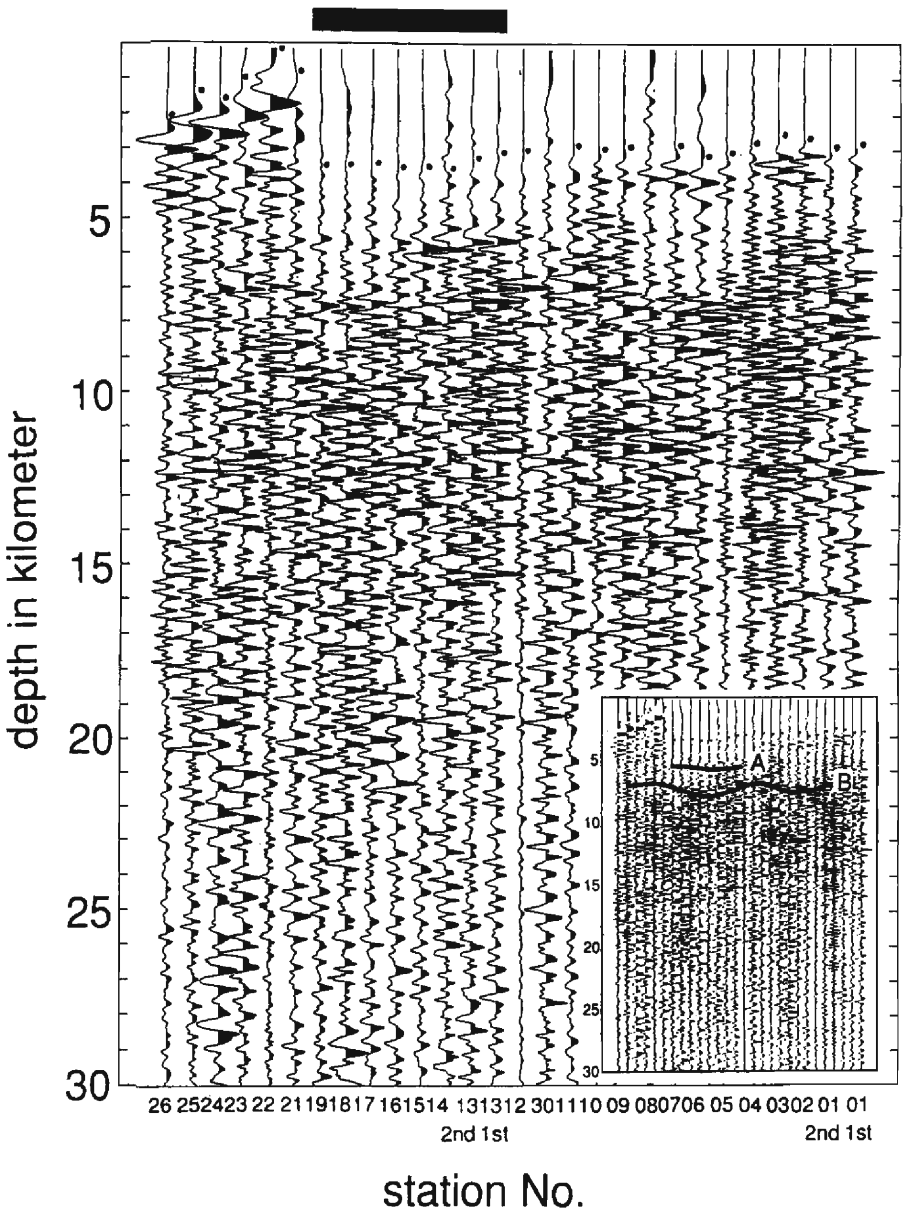

Fig. 7. Waveforms after NMO correction shown in azimuthal sequence; right to left, stations clockwise from the north. Records from the two shots are shown at stations 1 and 13. Dots denote the onset of initial P waves and the heavy line segment at the top indicates the extent of stations 13–19, where late P arrivals are observed. The inset shows two later phases *A* and *B*.

terns with the depth of some phases varying within about 1–2 km. When the three-layered structure model shown in **Fig. 4** is used, P arrivals at some stations were plotted at negative depths. Therefore, to prevent this, the result by using a semi-infinite structure with average P wave velocity of 3.8 km/s is shown as **Fig. 7**. First arrivals of refracted P waves after this kind of NMO correction are to be plotted at a depth of the boundary between the second and the third layer exactly for the three-layer model or near that boundary for the suitable half-space model. But the result plotted in **Fig. 7** shows a large offset from the expected depth. This is probably caused by the inadequacies of the structure model because we cannot estimate any velocity deeper than about 2 km. The depth of reflectors evaluated above should contain this kind of ambiguity. Furthermore, the first P arrivals plotted in the figure show large scattering in depth. This reflects the lateral heterogeneity of velocity structure such as the low-velocity region estimated above, the different thicknesses of the surface layer below the stations, and so on.

3. 4 Array data analysis

It can be evaluated whether coherent wave trains exist or not in the coda part and from which direction they propagate, by calculating the coherency of waveforms which is called the semblance (e.g., Neidell and Taner, 1971) for array observation data. The wave type of such propagating phases, body waves or surface waves, can be identified from the apparent slowness. The wave type for body waves, P or S waves, also can be identified by the analysis of a particle motion. Then the rough location of the secondary source of a given wave train will be estimated from the travel time measured from the shot time by assuming single scattering or single reflection. Nakamura et al. (1994) estimated the scatterer location by this method in the Kinki district, Japan.

Figure 8 shows the records of the first shot obtained at A1 array. The seismograms seem to contain a lot of later phases. The wave group about 0.6 sec after the P arrivals seen mainly in horizontal components can be interpreted as S waves from the shot, because they show a particle motion almost perpendicular to that of initial P waves. The seismograms for the second shot obtained at A2 array show much longer coda durations, the seismograms perhaps being strongly affected by the low-velocity sediment layer around the array site.

Figure 9 represents the temporal change of semblance computed from the vertical-component seismograms recorded at five stations of A1 array. Semblance was calculated for the slowness ranges less than 0.5 s/km for all directions and the maximum value among them has been plotted in the figure. The moving window length was taken as two times the center period (1/8 sec) of the band-pass filter used. The semblance of 1.0, the maximum value, means completely coherent waves arrive at the array from a certain direction and that of the minimum value, approximated by the reciprocal of the number of stations, means completely random waves coming from every direction. Direct P waves come from the direction of the shot point with large coherency. We can find several wave trains with large semblance values. Some of them may be interpreted as scattered or reflected waves from heterogeneous structures around the volcano.

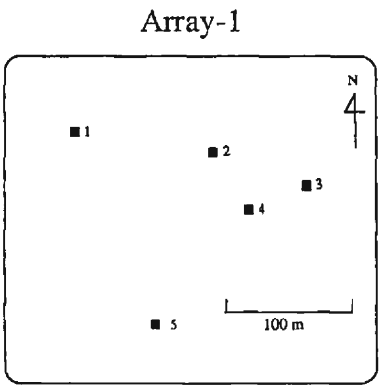

(a)

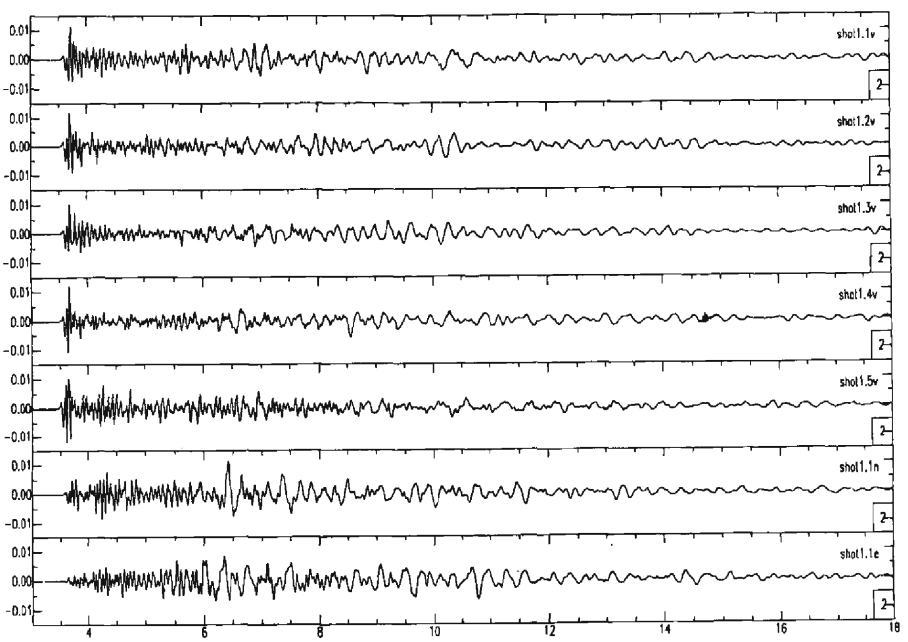

(b)

Fig. 8. (a) Configuration of five stations at A1 array located by a transit measurement. Three-component seismometers were installed at No. 1. (b) Seismograms from the first shot recorded at A1 array. Top to bottom : UD components at stations 1 to 5, NS and EW components at station 1. Horizontal axis indicates arbitrary time in sec, not measured from the shot time.

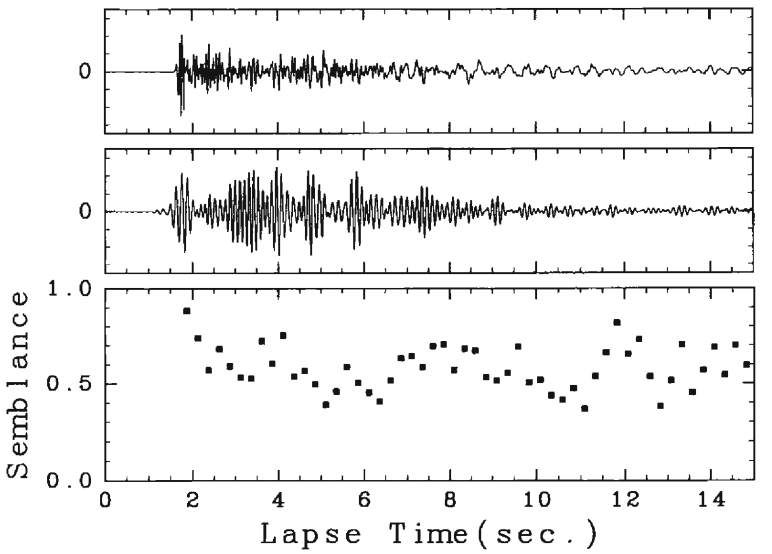

Fig. 9. Temporal change of semblance calculated from band–pass filtered waveforms (8 Hz) for A1 array. Lapse times are measured from the shot time. The original and filtered seismograms at station 5 are also shown.

4. Summary

We carried out a seismic explosion survey at Taal volcano employing the refraction, fan–shooting and reflection methods. By summarizing the results of these observations, a possible explanation of underground structure of Taal Volcano was obtained as shown in **Fig. 10**. While the location and extent cannot be determined exactly, a low–velocity and low–Q region

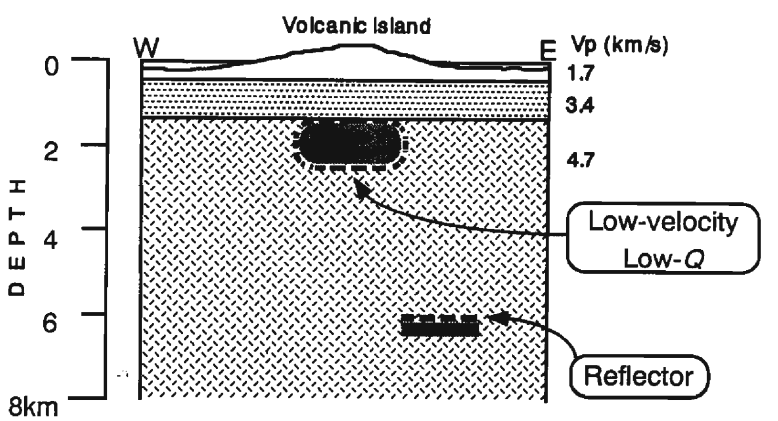

Fig. 10. Schematic illustration showing a possible explanation of structure, E–W vertical cross section below Taal Volvano.

exists around the main crater at a depth of about 1.5 km. P wave velocity of this abnormal region may be estimated to be lower than that of the surroundings by much greater than about 25%, if we assume the region is restricted just below the main crater. A reflector was detected eastward of the main crater at a depth of about 6 km, which may suggest the top surface of a magma reservoir.

The results obtained here contain large ambiguity because records from only one shot were analyzed. With the next survey, we plan to make another explosion at the southeast shore of Lake Taal and to deploy the fan-shooting stations along the northern part of lake shore.

Acknowledgement

We are grateful to Mr. T. Ikeda, first secretary of the Embassy of Japan, for giving us facilities for customs clearance at Manila International Airport. We wish also to thank Mr. H. Hatakeyama of Engineering Geophysics Research Institute, Oyo Corporation and Dr. K. Ito of Disaster Prevention Research Institute, Kyoto University for providing information about explosion and explosives. Valuable comments by Dr. T. Iwata of DPRI, Kyoto Univ. and an anonymous reviewer were helpful in improving the manuscript. This study was partly supported by a Grant-in-Aid for Scientific Research, No. 03041042, from the Ministry of Education, Science and Culture, Japan.

References

Achauer, U., J. R. Evans, and D. A. Stauber : High-resolution seismic tomography of compressional wave velocity structure at Newberry Volcano, Oregon Cascade Range, J. Geophys. Res., Vol. 93, 1988, pp. 10135–10147.

Achauer, U., L. Greene, J. R. Evans, and H. M. Iyer : Nature of the magma chamber underlying the Mono Crater area, eastern California, as determined from teleseismic travel time residuals, J. Geophys. Res., Vol. 91, 1986, pp. 13873–13891.

Ankeny, L. A., L. W. Braile, and K. H. Olsen : Upper crustal structure beneath the Jemez Mountains volcanic field, New Mexico, determined by three-dimensional simultaneous inversion of seismic refraction and earthquake data, J. Geophys. Res., Vol. 91, 1986, pp. 6188–6198.

Brown, L. D., C. E. Chapin, A. R. Sanford, S. Kaufman, and J. Oliver : Deep structure of the Rio Grande Rift from seismic reflection profiling, J. Geophys. Res., Vol. 85, 1980, pp. 4773–4800.

Cardwell, R. K., B. L. Isacks, and D. E. Karig : The spatial distribution of earthquakes, focal mechanism solutions, and subducted lithosphere in the Philippine and Northeastern Indonesian Islands, in The tectonic and geologic evolution of Southeast Asian Seas and Islands, Geophys. Monogr. Ser. 23, edited by D. E. Hayes, AGU, Washington, D. C., 1980, pp. 1–35.

Evans, J. R. and J. J. Zucca : Active high-resolution seismic tomography of compressional wave velocity and attenuation structure at Medicine Lake volcano, northern California Cascade Range, J. Geophys. Res., Vol. 93, 1986, pp. 15016–15036.

Hill, D. P., E. Kissling, J. H. Luetgert, and U. Kradolfer : Constraints on the upper crustal structure of the Long Valley–Mono Craters volcanic complex, eastern California, from seismic refraction measurements, J. Geophys. Res., Vol. 90, 1985, pp. 11135–11150.

Ishihara, K. : Geophysical evidences on the existence of magma reservoir and conduit at Sakurajima Volcano, Japan, Annuals Disas. Prev. Res. Inst. Kyoto Univ., No. 31B-1, 1988, pp. 59–73 (in Japanese).

Mikumo, T., K. Hirahara, F. Takeuchi, H. Wada, T. Tsukuda, I. Fujii, and K. Nishigami : Three-di-

mensional velocity structure of the upper crust in the Hida region, central Honshu, Japan, and its relation to Quaternary active faults and local seismicity, submitted to Tectonophysics, 1993.

Moriya, T. and H. Okada : Observation of a quarry blast in and around Usu Volcano : Travel time and Propagation anomaly caused by magma, Bull. Volcanol. Soc. Jpn., Vol. 52, 1980, pp. 63–74.

Nakamura, H., T. Iwata and K. Irikura : Estimation of scatterer distribution in the earth's crust using three–component small–aperture array observations, submitted to Bull. Seismol. Soc. Am., 1994.

Nakamura, K. : The magmatophreatic eruption of Taal Volcano in 1965, Philippines, Geology Magazine, 75, No. 2, 1966, pp. 93–104 (in Japanese).

Neidell, N. S. and M. T. Taner : Semblance and other coherency measures for multichannel data, Geophysics, Vol. 36, 1971, pp. 482–497.

Ono, K., K. Ito, I. Hasegawa, K. Ichikawa, S. Iizuka, T. Kakuta, and H. Suzuki : Explosion seismic studies in south Kyushu especially around the Sakurajima Volcano, J. Phys. Earth, Vol. 26 (suppl.), 1978, pp. s309–s319.

Ueki, S., H. Hamaguchi, T. Inamori, S. Horiuchi, A. Nishizawa, S. Hori, K. Nida, S. Matsumoto, I. Umetsu, Y. Sato, A. Hasegawa, H. Miyamachi, Y. Nishimura, T. Maekawa, A. Suzuki, J. Inoue, D. Nanang, M. Suzuki, A. Ito, Y. Sudo, M. Iguchi, and A. Takagi : Crustal structure beneath Bandai Volcano revealed by fan–shooting measurement, Tohoku–chiiki Saigaikagaku Kenkyuu, Vol. 26, 1990, 87–91 (in Japanese).

Zhao, D., A. Hasegawa, and S. Horiuchi : Tomographic imaging of P and S wave velocity structure beneath northeastern Japan, J. Geophys. Res., Vol. 97, 1992, pp. 19909–19928.